Optical Differentiator Based on an Integrated Sidewall Phase-Shifted Bragg Grating

Weifeng Zhang, *Student Member, IEEE*, Wangzhe Li, *Student Member, IEEE*, and Jianping Yao, *Fellow, IEEE*

***Abstract*— We report the implementation of an all-optical temporal differentiator based on an integrated phase-shifted Bragg grating (PSBG) in a compact single-mode silicon-on-insulator ridge waveguide. The integrated PSBG is designed to have a wide reflection notch by creating deep corrugations on the sidewalls of the ridge. The device is fabricated using a CMOS compatible process with 248-nm deep ultraviolet lithography. An experiment is performed. The use of the integrated PSBG for the implementation of an all-optical temporal differentiator is demonstrated.**

***Index Terms*— Silicon photonics, integrated Bragg grating, waveguide, optical differentiator, microwave photonics, optical signal processing.**

I. Introduction

INTEGRATED waveguide Bragg gratings are expected to play a significant role in future silicon-based optical communications and sensing systems [1]. Compared with a uniform Bragg grating, a phase-shifted Bragg grating (PSBG) with an ultra-narrow transmission band can find applications such as in narrowband filtering [2], optical sensing [3] and optical signal processing [4]. For example, the phase jump at the resonant frequency of a PSBG makes it possible for the implementation of an all-optical temporal differentiator, a fundamental building block for optical signal processing [4]. A PSBG can be fabricated in a fiber or in an optical waveguide. The method of using electron-beam lithography and reactive ion etching has been demonstrated in the fabrication of a PSBG on a silicon-on-insulator (SOI) platform [5], but its high fabrication cost prevents it from commercial applications. Another method is to use deep ultraviolet (DUV) lithography [6]–[8], which brings advantages such as high throughput and low cost. In [7], a uniform Bragg grating was realized by corrugating the sidewalls of the waveguide, either on the ridge or the slab. In [8], a narrow-band transmission filter based on a PSBG in an SOI waveguide was demonstrated, in which the grating was corrugated on the sidewalls of the strip waveguide. In a strip waveguide, the high refractive index contrast between the core (silicon, $n = 3.42$ at 1550 nm) and the cladding (silicon dioxide or air, $n = 1.52$ or 1.00 at 1550 nm) makes the light strongly confined in the core. Due to the small cross section of the strip waveguide, the vertical sidewalls of the waveguide would affect the field distribution of the confined light mode. The advantage of such a configuration is that a small periodic perturbation on the sidewalls can cause a considerably large coupling coefficient change, which makes it possible to obtain a strong grating. One major disadvantage is that the propagation loss is usually high, due to the scattering resulted from the sidewall roughness [9]. In contrast, a ridge waveguide typically has a much larger cross section, which will lower the interaction between the confined light and the sidewalls, thus has high potential in producing a PSBG with lower propagation loss and allowing higher fabrication tolerance.

On the other hand, an all-optical temporal differentiator, performing temporal differentiation of the complex envelope of an arbitrary optical waveform, is one of the basic processing blocks, which can find applications in signal processing [10], pulse shaping [11], [12], and pulse coding [13]. Different schemes have been proposed recently for the implementation of all-optical temporal differentiators. For example, an all-optical temporal differentiator can be implemented using a phase-shifted fiber Bragg grating [4] or a silicon microring resonator [14]–[17]. A temporal differentiator based on a phase-shifted fiber Bragg grating is relatively easy to implement, but its high sensitivity to environmental changes makes it unusable for practical applications or complicated packaging is needed to increase its stability. A silicon-microring-resonator-based temporal differentiator has the advantage of small footprint. However, the high thermo-optic coefficient of silicon (1.86×10^{-4} K^{-1}) and the high wavelength selectivity make the resonators susceptible to fluctuations in temperature [18]. In addition, optical coupling to the ring resonator is achieved by directional couplers. Controlling the coupling is crucial and requires an elaborate design in the coupling structure. Recently, a temporal differentiator using a silicon-based Mach-Zehnder Interferometer (MZI) was experimentally demonstrated [19]. Compared with an integrated grating, the structure based on an MZI is bulky, and the splitting ratios of the input and output Y-branches must be precisely controlled, which would decrease the fabrication tolerances.

In this letter, we report the implementation of an all-optical temporal differentiator based on an integrated PSBG in an SOI ridge waveguide. The grating is designed to have a wide

Manuscript received February 26, 2014; revised August 5, 2014; accepted September 1, 2014. Date of publication September 11, 2014; date of current version November 4, 2014. This work was supported in part by the Natural Sciences and Engineering Research Council of Canada through the CREATE Program and in part by the CMC Microsystems, Kingston, ON, Canada.

The authors are with the Microwave Photonics Research Laboratory, School of Electrical Engineering and Computer Science, University of Ottawa, ON K1N 6N5, Canada (e-mail: jpyao@eecs.uottawa.ca).

Color versions of one or more of the figures in this letter are available online at http://ieeexplore.ieee.org.

Digital Object Identifier 10.1109/LPT.2014.2357418

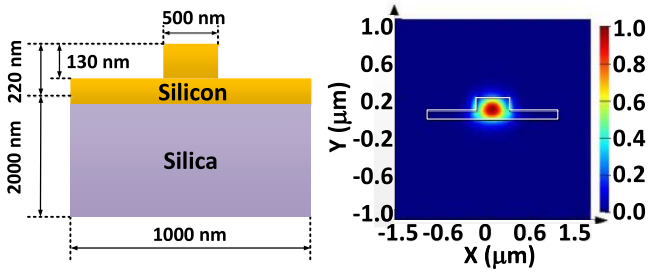

(a) (b)

Fig. 1. (a) Schematic diagram of the cross-section of the ridge waveguide. (b) Simulated fundamental TE mode profile in the ridge waveguide.

reflection notch, corresponding to a wide bandwidth of the temporal differentiator, by creating deep corrugations in the sidewalls in a compact single-mode SOI ridge waveguide. The device is fabricated using the standard CMOS compatible process with 248-nm deep ultraviolet lithography. An integrated PSBG, with a reflection notch having a width of approximately 0.3 nm (37.5 GHz), is fabricated. The device is then used for the implementation of a temporal differentiator. A Gaussian pulse with a bandwidth of 37.5 GHz is temporally differentiated.

II. Phase-Shifted Grating in an SOI Waveguide

First, the design of the waveguide and the integrated PSBG is performed. Fig. 1(a) illustrates the cross-section of the ridge waveguide on which a grating is fabricated. There is a top silicon layer of 220 nm in thickness and a bottom silica layer of 2 μm in thickness. The shallow-etched ridge width is 500 nm and the etch depth is 130 nm. The slab width is 1000 nm. The waveguide with the described dimensions supports single transverse-electric (TE) mode propagation.

A two-dimension simulation method [20] is applied to evaluate the optical mode distributions in the ridge waveguide. Fig. 1(b) shows the calculated mode profile of the fundamental TE mode in the ridge waveguide at 1550 nm. As shown in Fig. 1(b), most of the light is confined in the ridge and the distribution of the optical field around the sidewalls is very low, for both the ridge and slab sidewalls. Thanks to this low distribution, the propagation loss is reduced compared to a strip waveguide, since the propagation loss in a silicon waveguide mainly arises from the light scattering due to the sidewall roughness [21]. By creating corrugations in the sidewall of the ridge, a grating is achieved.

As shown in Fig. 2, the grating is realized by introducing periodic sidewall corrugations to the ridge. The grating period Λ is designed to be 320 nm, with a duty cycle of 60%, and the total length of the gratings is 1920 μm. A phase-shifted block, with a length of 160 nm corresponding to half of the grating period, to introduce a π phase shift, is allocated at the center of the grating. In the mask design, the shape of the corrugations is perfectly squared; however, the corrugations in a real fabricated grating are severely rounded due to the limited fabrication resolution. Therefore, a larger corrugation depth is used in the mask design to obtain a coupling coefficient that is identical to that of the designed grating.

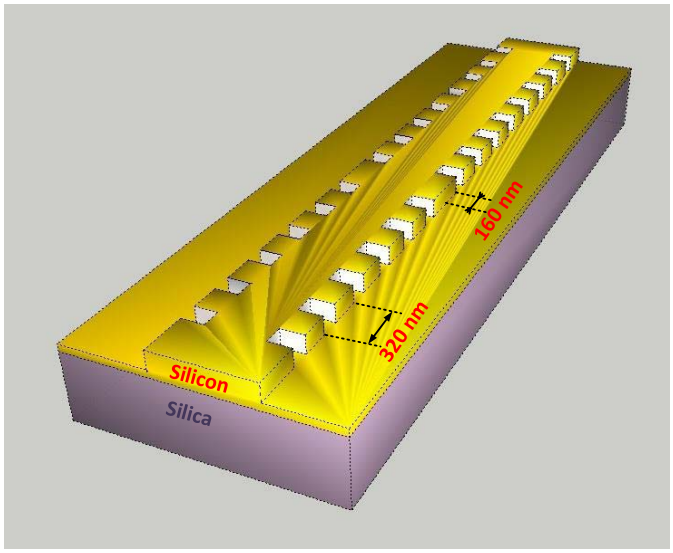

Fig. 2. Configuration of the PSBG in a SOI ridge waveguide.

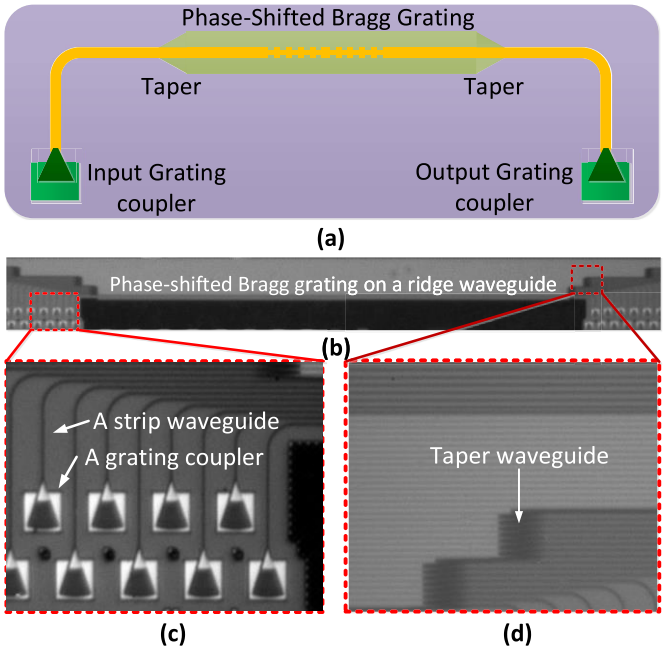

Fig. 3. (a) Schematic layout of the designed device. (b) Image of the fabricated device obtained from a microscope camera. (c) Image of the grating couplers and the strip waveguides. (d) Image of a taper waveguide for the transition between a strip waveguides and a ridge waveguide.

Fig. 3(a) shows the layout of the designed device. At the two ends of the grating there are two integrated waveguide-to-fiber grating couplers, which are used to couple the light wave into and out of the chip. To minimize the chip footprint and to reduce the bending loss, a strip waveguide is incorporated in the design to guide the light wave from the input grating coupler to the PSBG and from the PSBG to the output grating coupler. Since the PSBG is in the ridge waveguide, a double-layer linear taper waveguide of a length of 50 μm is designed to achieve the transition between the strip and the ridge waveguides. Fig. 3(b) shows a microscopic image of the

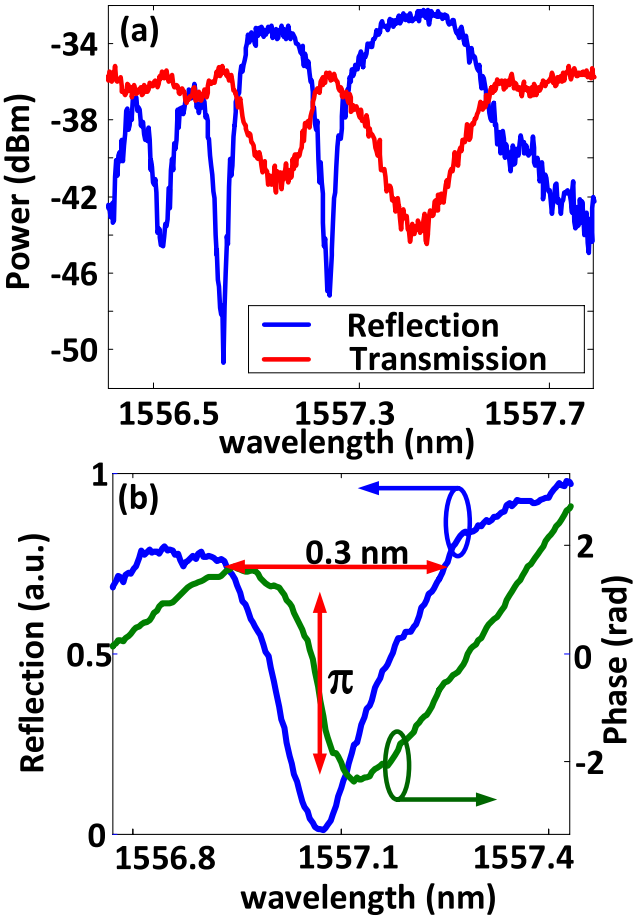

Fig. 4. (a) Measured reflection and transmission spectral responses of the fabricated PSBG on a ridge waveguide with a designed corrugation depth of 125 nm. (b) Zoom-in view of the reflection notch and its phase response.

fabricated device obtained from a microscope camera. Fig. 3(c) shows the microscopic images of the grating couplers and the strip waveguides, and Fig. 3(d) shows the microscopic image of the taper waveguides for the transition between the strip waveguides and ridge waveguides.

The spectral response of the fabricated device is measured using an optical vector analyzer (LUNA OVA CTe). The reflection and transmission spectra of the integrated PSBG, of which the corrugation depth is 125 nm in the mask design, are shown in Fig. 4(a). It can be seen there is a resonant transmission window within the stop band in the transmission spectrum. The measured Bragg wavelength is at about 1557 nm, which is shorter than the value of 1580 nm in the design. The blue shift of the Bragg wavelength is caused by the fact that the fabricated waveguide has a lower effective refractive index than the designed waveguide due to the fabrication imperfection. To ensure the grating to work at the designed Bragg wavelengths, the fabrication imperfections should be taken into consideration in the selection of the grating period. Note that a grating on a ridge waveguide is usually has a smaller transmission bandwidth than a grating on a strip waveguide if all design parameters are controlled identical. However, in our design, in order to implement an all-optical temporal differentiator with a wide bandwidth, the

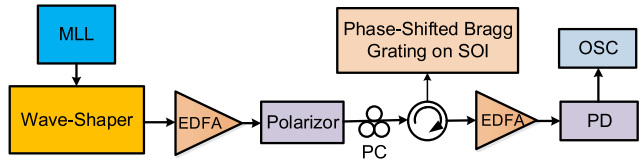

Fig. 5. Experimental setup. MML: mode lock laser. EDFA: erbium-doped fiber amplifier. PC: polarization controller. PD: photodetector. OSC: oscilloscope.

grating is deliberately designed to have a wide reflection notch by increasing the depth of the corrugations. As shown in Fig. 4(b), the width of the reflection notch (top-to-top width) of the fabricated PSBG is approximately 0.3 nm (or 37.5 GHz). The phase response is also shown in Fig. 4(b). It is clearly seen that a phase jump of π at the Bragg wavelength is produced. The PSBG with such a spectral response can be used in the implementation of an all-optical temporal differentiator with an operation bandwidth of 37.5 GHz.

III. All-Optical Temporal Differentiator

The use of the fabricated integrated PSBG to perform the first-order temporal differentiation of an optical waveform is studied. A first-order temporal differentiator provides the first-order temporal derivative of the complex envelope of an input optical signal. A temporal differentiator can be considered as a linear time-invariant (LTI) system with a frequency response given by

$$H(\omega) = j(\omega - \omega_0) = \begin{cases} |\omega - \omega_0| e^{j\frac{\pi}{2}}, & \omega > \omega_0 \\ |\omega - \omega_0| e^{-j\frac{\pi}{2}}, & \omega < \omega_0 \end{cases} \quad (1)$$

where ω is the optical angular frequency and ω_0 is the angular frequency of the optical carrier.

As can be seen from (1), a first-order all-optical temporal differentiator can be implemented using an optical filter that has a magnitude response of $|\omega - \omega_0|$ and a phase response of $\pi/2$ for $\omega > \omega_0$ and $-\pi/2$ for $\omega < \omega_0$ corresponding to a phase jump of π at ω_0. The frequency response of the PSBG at the reflection notch is close to that of the optical filter given by (1), thus a first-order all-optical temporal differentiator can be implemented using the PSBG.

An experiment is performed to evaluate the operation of the PSBG as a temporal differentiator. The experimental setup is shown in Fig. 5. A mode-locked laser (MLL) is used to generate a short Gaussian pulse with a temporal full-width at half-maximum (FWHM) of 550 fs, centered at 1558.5 nm. A WaveShaper (Finisar 4000S) is connected after the MLL to extend the temporal FWHM of the Gaussian pulse to 24 ps (corresponding to a spectral width of 37.5 GHz) centered at 1557.05 nm. An erbium-doped fiber amplifier (EDFA) connected at the output of the WaveShaper is used to compensate for the insertion loss of the system. A polarizer (Pol) is used to make the light wave from the EDFA linearly polarized, and a polarization controller (PC) connected to the Pol is used to control the polarization state of the input light to the PSBG. Two lensed fibers are used, one is to couple the light into the chip and the other is to collect the

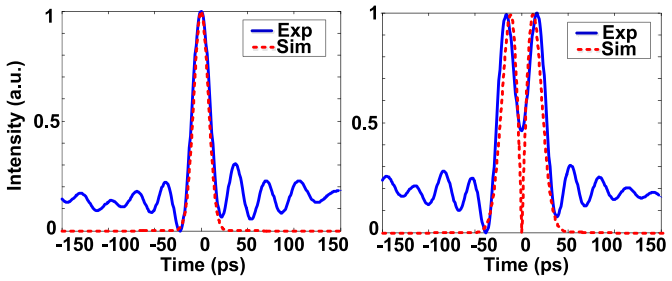

Fig. 6. (a) An input Gaussian pulse with an FWHM of 25 ps, and (b) the temporally differentiated pulses by simulation and experiment.

transmitted light from the chip. A second EDFA is employed to amplify the reflected light wave. The temporally differentiated signal is detected by a photodetector (PD, New Focus, 45 GHz bandwidth) and its waveform is observed by a real-time oscilloscope (OSC, Agilent DSO-X93204A).

Fig. 6(a) shows the Gaussian pulse (blue-solid line) at the output of the WaveShaper. A simulated Gaussian pulse (red-dashed line) is also shown for comparison. The ripples observed at the tails of the measured Gaussian pulse are resulted from the OSC due to the limited sampling rate. Fig. 6(b) shows the corresponding temporally differentiated pulse (blue-solid line). Again, a simulated temporally differentiated pulse (red-dashed line) is also shown for comparison. As can be seen the experimentally generated pulse is close to the simulated pulse, which confirms the effectiveness of the use of the PSBG to perform a first-order temporal differentiator. Some ripples are observed in the experimentally generated pulse, which are again resulted from the OSC due to the limited sampling rate. We also note that the dip in the center of the experimentally differentiated pulse is not as deep as the simulated pulse, which is mainly caused by the limited bandwidth of the PD (45 GHz).

IV. Conclusion

We have demonstrated the implementation of an all-optical temporal differentiator based on an integrated PSBG in a compact single-mode SOI ridge waveguide. The integrated PSBG was designed to have a wide reflection notch by creating the deep corrugations on the sidewalls of the ridge. The device was fabricated using a CMOS compatible process with 248-nm deep ultraviolet lithography. An integrated PSBG with a reflection notch having a width of approximately 0.3 nm was fabricated, which was then used for the implementation of temporal differentiator. The temporal differentiation of a Gaussian pulse with a bandwidth of 37.5 GHz was experimentally demonstrated.

References

[1] T. E. Murphy, J. T. Hastings, and H. I. Smith, "Fabrication and characterization of narrow-band Bragg-reflection filters in silicon-on-insulator ridge waveguides," *J. Lightw. Technol.*, vol. 19, no. 12, pp. 1938–1942, Dec. 2001.

[2] G. P. Agrawal and S. Radic, "Phase-shifted fiber Bragg gratings and their application for wavelength demultiplexing," *IEEE Photon. Technol. Lett.*, vol. 6, no. 8, pp. 995–997, Aug. 1994.

[3] F. Kong, W. Li, and J. Yao, "Transverse load sensing based on a dual-frequency optoelectronic oscillator," *Opt. Lett.*, vol. 38, no. 14, pp. 2611–2613, Jul. 2013.

[4] N. K. Berger, B. Levit, B. Fischer, M. Kulishov, D. V. Plant, and J. Azaña, "Temporal differentiation of optical signals using a phase-shifted fiber Bragg grating," *Opt. Exp.*, vol. 15, no. 2, pp. 371–381, Jan. 2007.

[5] H.-C. Kim, K. Ikeda, and Y. Fainman, "Tunable transmission resonant filter and modulator with vertical gratings," *J. Lightw. Technol.*, vol. 25, no. 5, pp. 1147–1151, May 2007.

[6] I. Giuntoni *et al.*, "Deep-UV technology for the fabrication of Bragg gratings on SOI rib waveguides," *IEEE Photon. Technol. Lett.*, vol. 21, no. 24, pp. 1894–1896, Dec. 15, 2009.

[7] X. Wang, W. Shi, H. Yun, S. Grist, N. A. F. Jaeger, and L. Chrostowski, "Narrow-band waveguide Bragg gratings on SOI wafers with CMOS-compatible fabrication process," *Opt. Exp.*, vol. 20, no. 14, pp. 15547–15558, Jun. 2012.

[8] X. Wang, W. Shi, S. Grist, H. Yun, N. A. F. Jaeger, and L. Chrostowski, "Narrow-band transmission filter using phase-shifted Bragg gratings in SOI waveguide," in *Proc. IEEE Photon. Conf.*, Oct. 2011, pp. 869–870.

[9] K. K. Lee, D. R. Lim, L. C. Kimerling, J. Shin, and F. Cerrina, "Fabrication of ultralow-loss Si/SiO_2 waveguides by roughness reduction," *Opt. Lett.*, vol. 26, no. 23, pp. 1888–1890, Dec. 2001.

[10] F. Li, Y. Park, and J. Azaña, "Complete temporal pulse characterization based on phase reconstruction using optical ultrafast differentiation (PROUD)," *Opt. Lett.*, vol. 32, no. 22, pp. 3364–3366, Nov. 2007.

[11] J. P. Yao, F. Zeng, and Q. Wang, "Photonic generation of ultrawideband signals," *J. Lightw. Technol.*, vol. 25, no. 11, pp. 3219–3235, Dec. 2007.

[12] Y. Park, M. Kulishov, R. Slavík, and J. Azaña, "Picosecond and sub-picosecond flat-top pulse generation using uniform long-period fiber gratings," *Opt. Exp.*, vol. 14, no. 26, pp. 12670–12678, Dec. 2006.

[13] J. A. N. da Silva and M. L. R. de Campos, "Spectrally efficient UWB pulse shaping with application in orthogonal PSM," *IEEE Trans. Commun.*, vol. 55, no. 2, pp. 313–322, Feb. 2007.

[14] Y. Hu *et al.*, "An ultra-high-speed photonic temporal differentiator using cascaded SOI microring resonators," *J. Opt.*, vol. 14, no. 6, pp. 065501–065508, Apr. 2012.

[15] G. Zhou *et al.*, "All-optical temporal differentiation of ultra-high-speed picosecond pulses based on compact silicon microring resonator," *Electron. Lett.*, vol. 47, no. 14, pp. 814–816, Aug. 2011.

[16] F. Liu, T. Wang, L. Qiang, T. Y. Zhang, M. Qiu, and Y. Su, "Compact optical temporal differentiator based on silicon microring resonator," *Opt. Exp.*, vol. 16, no. 20, pp. 15880–15886, Sep. 2008.

[17] H. Shahoei, D.-X. Xu, J. H. Schmid, and J. Yao, "Photonic fractional-order differentiator using an SOI microring resonator with an MMI coupler," *IEEE Photon. Technol. Lett.*, vol. 25, no. 15, pp. 1408–1411, Aug. 1, 2013.

[18] M. S. Nawrocka, T. Liu, X. Wang, and R. R. Panepucci, "Tunable silicon microring resonator with wide free spectral range," *Appl. Phys. Lett.*, vol. 89, no. 7, pp. 071110-1–071110-4, Aug. 2006.

[19] J. Dong, A. Zheng, D. Gao, L. Li, D. Huang, and X. Zhang, "Compact, flexible and versatile photonic differentiator using silicon Mach–Zehnder interferometers," *Opt. Exp.*, vol. 21, no. 6, pp. 7014–7024, Mar. 2013.

[20] *Software: MODE Solutions*, Lumerical Solutions, Inc., Vancouver, BC, Canada, 2003.

[21] P. Dong *et al.*, "Low loss shallow-ridge silicon waveguides," *Opt. Exp.*, vol. 18, no. 14, pp. 14474–14479, Jul. 2010.